



Investigation on Microstructure and Mechanical Properties of TA10–Q245R Composite Plate Formed by Explosive Welding

Shaogang Wang and Xiaomin Han

(Submitted September 22, 2017; in revised form May 4, 2019; published online July 8, 2019)

The titanium alloy TA10 and the carbon steel Q245R are welded by explosive welding, and post-weld heat treatment (PWHT) is carried out for the TA10–Q245R composite plate. Microstructure and mechanical properties of the composite plate are investigated both in as-welded (AW) condition and after PWHT, respectively. Results show that, in AW condition, the bonding interface of composite plate presents wavy morphology, and at both sides of the interface plastic deformation is generated to a certain degree. Near the interface interdiffusion zone of alloying elements exists, and no Fe–Ti intermetallic compound is produced at the interface. SEM images indicate that the tensile fracture of composite plate presents the characteristic of ductile fracture, and no defects such as gas pores or impurities are found on the surface of shear fracture. After PWHT, the interfacial microstructure of the composite plate is obviously changed. Compared with the mechanical properties of the composite plate in AW condition, both tensile strength and shear strength of the composite plate are decreased to a certain extent after PWHT. With various factors into consideration, the suitable heat treatment procedure of TA10–Q245R composite plate is determined as follows: 550 °C × 1.5 h.

Keywords explosive welding, heat treatment, interfacial microstructure, mechanical properties, titanium–steel composite plate

1. Introduction

The TA10 is a near α -type titanium alloy containing low contents of alloying elements, which belongs to one of the Ti–Mo–Ni series. It has good mechanical property at high temperature and better crevice corrosion resistance to chloride with low pH value or acid with weak reducibility. Its corrosion resistance is obviously better than that of pure titanium, so it is widely used in petrochemical industry, etc. The carbon steel Q245R has high stiffness, well matching between strength and toughness, and low price, so it is widely used in the field of petrochemical industry, power station equipment, boiler and pressure vessel, etc. If the TA10 and the Q245R are combined through a suitable technological process, the obtained titanium–steel composite plate may be employed to make equipment with excellent comprehensive properties: the good corrosion resistance of titanium alloy and the high strength of carbon steel. Therefore, the production cost can be greatly reduced, and the market competitiveness of product can be greatly increased.

However, the reaction will occur between titanium and steel at high temperature, and several types of intermetallic compounds will be formed. Consequently, it is difficult to weld them together by using common fusion welding process.

Explosive welding is one of the common ways to fabricate metal composite plates. During explosive welding, the dynamite causes oblique impact at high speed between base metal and flyer metal. A thin transition layer with plastic deformation, local fusion, elements diffusion and wavy feature are produced at the interface, which results in firm bonding between the base plate and the flyer plate. The remarkable characteristic of explosive welding is that similar metals (Ref 1–3) or dissimilar metals (Ref 4, 5) could be welded directly. Up to now, explosive welding has been successfully applied to many materials, including metals and nonmetals. Explosive composite materials have been widely used in petrochemical industry, pressure vessel, shipbuilding, aerospace and nuclear industry (Ref 6–8).

At present, the explosive welding process of titanium–steel (Ref 9–11), titanium–stainless steel (Ref 12–16), copper–steel (Ref 17) and copper–stainless steel (Ref 18, 19), etc., and their microstructure and mechanical properties of composite plates (Ref 20, 21) had been investigated by many researchers, and great progress had been made. Rao et al. (Ref 22) studied the interfacial microstructure of explosive composite plate between pure titanium and high-strength low-alloy (HSLA) steel. Results showed that there was a small amount of melted layer at the wave peak of the interface, and its composition was based on titanium and HSLA steel. Maliutina et al. (Ref 23, 24) reported that the interface presented an obvious wavy morphology, and the addition of interlayer (bronze–tantalum) could effectively eliminate crack caused by intermetallic compound at the interface of titanium–stainless steel composite plate. PWHT was conducted to the composite plate at heating temperature of 500, 600, 700 and 800 °C for 1 h, respectively. Results showed that the microstructure did not change obviously at the side of stainless steel during heat treatment, because the heating temperature did not exceed its recrystallization temperature. Jiang et al. (Ref 25) found that the atomic diffusion at the

Shaogang Wang and Xiaomin Han, College of Material Science and Technology, Nanjing University of Aeronautics and Astronautics, Nanjing 211106, China. Contact e-mail: sgwang@nuaa.edu.cn.

interface could be promoted by heat treatment. However, when the heating temperature was over 850 °C, a lot of Ti-Fe intermetallic compounds would be formed at the interface, which resulted in the significant decrease in shear strength of the composite plate.

Yadegari et al. (Ref 26) investigated the effect of heat treatment on interfacial microstructure and bonding strength of Ti-304L composite plate. Results showed that the σ and Fe₂Ti phases would be generated at the interface at heating temperature of 700 °C. With the elevation of heating temperature, the other intermetallic compounds such as λ , FeTi, NiTi and NiTi₂ were also generated at the interface. Zhang et al. (Ref 27) studied the effect of aging treatment on mechanical properties of beryllium bronze-carbon steel composite plate. Deng et al. (Ref 28) revealed the interfacial microstructure of aluminum-stainless steel composite tube, and the corresponding analysis was carried out based on explosive welding procedure and loading course of explosion. Muneshwar et al. (Ref 29) explored the effect of different procedures on the welding of aluminum-stainless steel composite plate. When a pure aluminum plate was used as the transition layer, the formation of intermetallic compound could be greatly inhibited. Acarer (Ref 30) prepared aluminum-copper transition joint by explosive welding and analyzed the electrical conductivity, electrochemical corrosion resistance and mechanical properties of the transition joint.

In recent years, the application of explosive welding is gradually expanded. The explosive welding of dissimilar metals such as titanium-steel, copper-steel and titanium-aluminum (Ref 31, 32) had been carried out previously. Some findings had been gotten, involving explosive welding procedure and welding parameters optimization, microstructure analysis and property tests of composite plate, PWHT of composite plate, etc. According to the literature report, the flyer plate for titanium-steel composite plate is mainly pure titanium at present. However, the strength of pure titanium is decreased with the elevation of temperature. When the temperature is over 250 °C, its tensile strength is reduced by half. In order to enlarge the application of titanium-steel composite plate at high temperature and corrosion environment, it is necessary to investigate systematically the explosive welding of TA10-Q245R composite plate. There is no relevant report on the explosive welding of this composite plate. Therefore, the

present work aims at the microstructure and mechanical properties of TA10-Q245R composite plate in AW condition, as well as the effect of different heat treatment procedures on microstructure and mechanical properties, so as to provide some guidance for practical application of this composite plate.

2. Experimental Materials and Procedure

The flyer plate is the annealed titanium alloy TA10 with the thickness of 3 mm, and the base plate is the hot-rolled carbon steel Q245R with the thickness of 12 mm. Their chemical compositions are given in Tables 1 and 2, respectively. The low limit values of tensile strength for TA10 and Q245R are 345 and 400 MPa, respectively. Before welding, the surfaces of plates are thoroughly cleaned. Firstly, they are polished with sand paper, then cleaned with acetone and dried. According to National Standard of the People's Republic of China GB/T 8547-2006 "Titanium clad steel plate", the TA10-Q245R composite plate is welded by explosive welding. Normally, the explosive welding parameters involve the pattern of placement, types of dynamite, ignition mode, stand-off distance between base plate and flyer plate, thickness of dynamite, detonation velocity, etc. The determination of each welding parameter is based on the characteristic and dimension of experimental plates. The detailed explosive welding parameters are given in Table 3.

After explosive welding, the samples are cut from the composite plate along explosion direction. The interfacial microstructure of the composite plate is observed by using MM6 type optical microscope. For the preparation of metallographic observation samples, the appropriate etchants need to be chosen, respectively, to etch different sides of the composite plate, because there is great difference in chemical composition and physical and chemical properties between the TA10 and the Q245R. The 4% Nital is used to etch the side of Q245R firstly, and then, the Kroll reagent whose proportion of ingredients is HF:HNO₃:H₂O = 3:2:95 is used to etch the side of TA10. The phase constituent of composite plate interface is inspected by using D8 Advance type x-ray diffractometer. The tensile strength and shear strength of composite plate are measured by using CMT5105 type electron universal machine with the maximal loading

Table 1 Chemical composition of titanium alloy TA10 (wt.%)

Mo	Ni	O	C	N	H	Fe	Ti
0.20-0.40	0.60-0.90	≤ 0.30	≤ 0.08	≤ 0.03	≤ 0.015	≤ 0.30	Bal.

Table 2 Chemical composition of carbon steel Q245R (wt.%)

C	Si	Mn	P	S	Al	Fe
≤ 0.20	≤ 0.35	0.50-1.00	≤ 0.025	≤ 0.015	≥ 0.02	Bal.

Table 3 Explosive welding parameters of TA10-Q245R composite plate

Placement pattern	Types of dynamite	Ignition mode	Stand-off distance <i>H</i> , mm	Thickness of dynamite <i>h</i> , mm	Detonation velocity <i>V</i> , m/s
Parallel placement	Mixed powder dynamite	Ignited at edge	3.0	24.0	2200-2400

capacity of 100 kN. The bending tests are carried out for the composite plate by using WE-300 type hydraulic universal material testing machine. The microhardness distribution of the composite plate interface is measured by using HVS-1000 type Vickers hardness tester. The morphologies of tensile fracture and shear fracture, and distribution of alloying elements at the interface are observed and analyzed by using Quanta 200 type scanning electron microscope (SEM) and energy-dispersive spectrometer (EDS), respectively. The substructure of the composite plate interface is investigated by using FEI Tecnai G2 type transmission electron microscope (TEM). Heat treatment is conducted to TA10–Q245R composite plate with different annealing processes, and microstructure analyses and mechanical properties tests are carried out for the composite plate after PWHT. The effect of different heat treatments on microstructure and mechanical properties of the composite plate is investigated; thus, the optimized heat treatment procedure is determined under the experimental condition.

3. Results and Discussion

3.1 Interfacial Microstructure of Composite Plate in AW Condition

3.1.1 Metallurgical Structure of Interface. The interfacial microstructure of the composite plate in AW condition is shown in Fig. 1. It presents the obvious wavy bonding at the

interface (Ref 11) with periodic cycle along explosion direction, as shown in Fig. 1(a). In general, there are three types of interfaces for composite plate after explosive welding, namely straight, wavy and melted layer (Ref 33). The effective bonding area with wavy interface between the base plate and the flyer plate increases, and the bonding strength with wavy interface is usually higher than that with straight interface.

During explosive welding, plastic deformation will occur to the metals of bonding zone under the action of explosion load. The microstructure of composite plate at the side of Q245R is shown in Fig. 1(b). It can be seen that the deformation degree of grains is different in different zones. Even if in the same zone, deformation also varies with the distance away from the interface. The microstructure from the interface to the base metal can be divided into the following zones: fine-grain zone, deformation streamline zone and original microstructure zone. Generally, the explosion pressure is the highest in fine-grain zone due to the shortest distance to the interface, which results in severe plastic deformation (Ref 12), and crystals are broken to form fine-grain zone. Moreover, the heat generated by plastic deformation induces recrystallization of structure at the interface; thus, the grain is refined. For the formation of streamline structure, on the one hand, it is under the action of stretching caused by severe plastic deformation; on the other hand, recovery occurs to the lath-shaped structure under the action of interfacial heat, and grains combine together and grow. With the distance away from the interface, the effect of explosion load is gradually decreased, and microstructure tends to be the original structure of base metal.

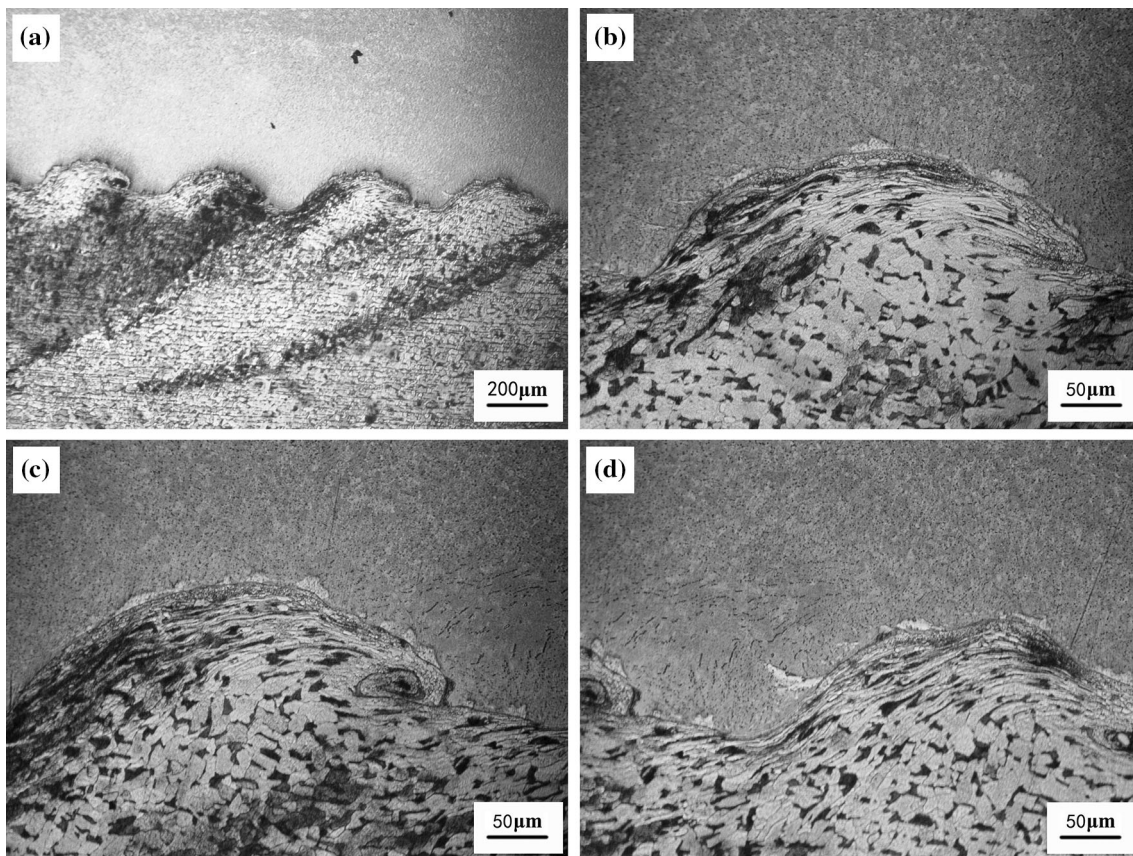


Fig. 1 (a) Wavy interface, (b) microstructure at the side of Q245R, (c) vortex, (d) discontinuous melted layer in wave trough

Periodic swing occurs to the metal jet during explosive welding. If the metal jet is deflected downward, and it is whirled by the coming fluid of base plate, as a result, the front vortex will be formed, as shown in Fig. 1(c). Gas poles, micro-crack, impurity, etc., are easily produced in vortex. Usually, the formation and dimension of vortex are greatly influenced by interfacial wavelength. If the wavelength is shorter, the dimensions of front and back vortex will be smaller, even no vortex is formed. In the case, the interfacial bonding strength is higher. Therefore, the explosive welding parameter is critical to determine the wavelength, and the high impact velocity and large dimension of vortex will result in the decrease in interfacial bonding strength.

The melted layer distributed discontinuously at the interface can be found in Fig. 1(c) and (d). As described in the literature (Ref 13), local melted zone existed at the interface. During explosive welding, if the gas does not fully escape from the gap between base plate and flyer plate, the residual gas will be adiabatically compressed at the interface; thus, a thin layer metal will be molten around the gas. The formation of melted layer can be divided into the following stages: (1) residual gas does not escape due to restriction around the wavy bonding zone during welding; (2) residual gas is adiabatically compressed under the action of instantaneous high pressure and high speed; (3) energy from extra load converts into thermal energy after residual gas is compressed, and the heat makes the base metal melted around gas. When the gas is compressed to be flat, the molten metal will become continuous or discontinuous melted layer after crystallization.

3.1.2 TEM Analysis of the Interface. TEM analysis of the composite plate interface is carried out. The TEM specimen is prepared at the following steps: mechanically grinding to the thickness of 40-60 μm , then punching thin foils with the diameter of 3 mm, and thinning with argon ion beam. The morphology of the interface is shown in Fig. 2, and the left side is TA10, and the right side is Q245R. It can be seen that the

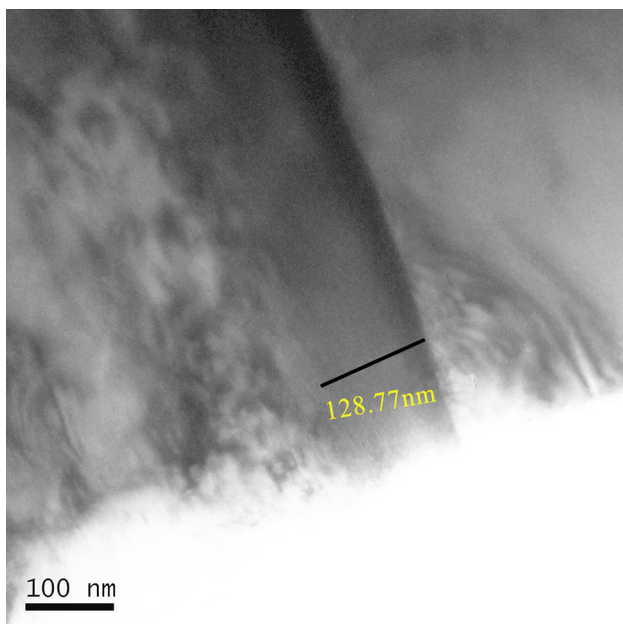


Fig. 2 TEM image of interface for TA10–Q245R composite plate

width of the interface is about 128.77 nm. During explosive welding, severe plastic deformation occurs at the side of TA10 due to the action of explosion load. Subsequently, it impacts to base plate Q245R and the metal jet is generated. The jet can help to clean the surface of the base plate, and the atomic distance between the base plate and the flyer plate is achieved, which is advantageous for attraction to each other and element diffusion. The bonding interface is thus formed, which mainly presents the direct connection with the solid phase. The intermetallic compound is not found at both sides of the composite plate interface.

Moreover, floccule occurs at both sides of the metals near the interface, which are dislocations within grains. The dislocation density at the side of TA10 is higher than that at the side of Q245R. The reason is probably that dynamic bending occurs to the flyer plate under the action of explosive load, and the flyer plate strongly impacts the base plate. Both of these two processes will increase the dislocation density within grains due to plastic deformation. There is stable high-temperature phase β in TA10, and its softening temperature is higher than that of Q245R. The metals at both sides of the interface will be softened due to the heat generated by explosive welding. At the same temperature, the softening effect of TA10 is weaker than that of Q245R; thus, the dislocation density within grain of TA10 is higher than that of within Q245R.

The substructure of the composite plate near the interface is shown in Fig. 3. The obvious twin deformation occurs near the interface, and there are a lot of dislocations within the twins, as shown in Fig. 3(a). When the dislocations tangle one another during their movement, which makes slip deformation difficult, the twin deformation will be generated. As a complementary way of metal slip deformation, the twin plays an important role in the plastic deformation of metals. The formation of twins indicates that the deformation mechanism of metals is mainly the twin deformation near the interface during explosive welding. Substructure at the side of Q245R, a little away from the interface, is shown in Fig. 3(b). The residual trace of slip dislocation can be seen from Fig. 3(b), while the trace of the twin cannot be found. It demonstrates that the deformation mechanism, a little away from the interface, is mainly the slip. The dislocation density in this region is lower than that at the interface. Due to the weakening effect of explosion load, microstructure tends to be the original structure of the base metal.

3.2 Phase Constituent and Distribution of Alloying Elements of Interface in AW Condition

3.2.1 Phase Constituent of Interface. During explosive welding of dissimilar metals, the local fusion will occur at the interface under high temperature and high pressure. Moreover, the content of carbon element is higher in the base plate, and it is easy to diffuse at high temperature. As a result, the compound or intermediate phase is probably produced at the interface. Intermetallic compounds are usually hard and brittle, and they will do harm to the interfacial property of composite plate. Consequently, it is necessary to inspect the phase constituent of the interface. XRD curve of the composite plate interface is shown in Fig. 4. Main phases include α -Ti, β -Ti and α -Fe, and no intermediate phase such as FeTi and Fe₂Ti is found (Ref 13). Although the melted layer is formed (Fig. 1c and d), the existence of melted layer does not mean surely the

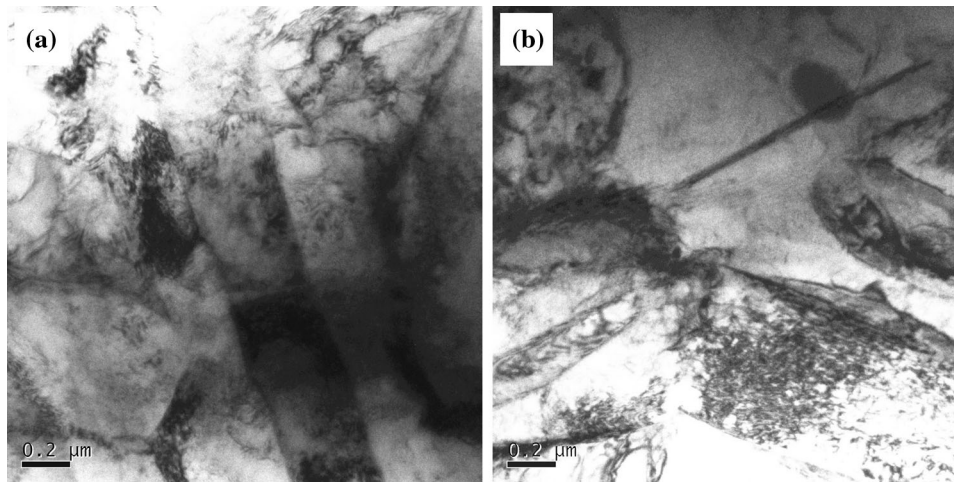


Fig. 3 (a) Twins at the side of TA10, (b) substructure at the side of Q245R a little away from interface

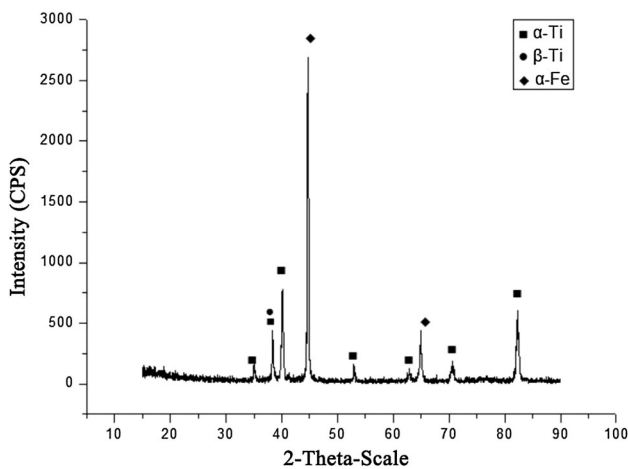


Fig. 4 XRD analysis of interface of TA10-Q245R composite plate

formation of intermetallic compound. On the other hand, the content of compound is so low, and the intensity of diffraction peak is so weak that it cannot be detected. It further demonstrates that the explosive welding process used in the present work is feasible, and the bonding strength of composite plate is high.

3.2.2 Distribution of Alloying Elements at Interface. Although the explosive welding time is very short, atomic diffusion occurs at the interface under high temperature and high pressure. Appropriate diffusion of alloying elements is advantageous to the interfacial bonding strength. The distribution of main alloying elements Fe and Ti is characterized by EDS, and the curves are shown in Fig. 5. The contents of elements Ti and Fe are obviously changed at the interface, as shown in Fig. 5(a). The sharp variation point of element concentration is not found except for at the interface. It demonstrates that segregation of elements Ti and Fe does not appear near the interface, and the distribution is relatively uniform. Figure 5(b) shows the obvious interdiffusion between elements Ti and Fe, and the diffusion distance is within micrometers.

The reason for diffusion of alloying elements at the interface is as follows: (1) high concentration gradient: During explosive welding of dissimilar metals, there exists great difference of concentration at both sides of the interface, which is the main driving force for diffusion of alloying elements with such a high concentration gradient. (2) Severe plastic deformation and local fusion of metal: During explosive welding, severe irreversible plastic deformation occurs at the interface under the action of explosion load. Plastic deformation results in a lot of dislocations and atom voids at high temperature, which causes interdiffusion of alloying elements. Crystal structure is damaged in molten state, and bonding force among atoms is decreased greatly, which is advantageous to interdiffusion of different atoms. (3) High temperature and high pressure: During explosive welding, much heat is generated by plastic deformation, which results in the elevation of temperature at the interface; thus, the diffusion of atoms is accelerated. With the elevation of temperature, the movement ability of atoms is enhanced and the amplitude of vibration is increased. The possibility for atoms to leave equilibrium position is greatly increased; thus, the atomic diffusion becomes easy. In addition, during explosive welding, the interfacial pressure greatly increases under the action of explosion load, and the high pressure results in strong diffusion of the alloying elements at the interface.

Because the explosive welding time is very short, the diffusion time of atoms is also very short. Thus, the diffusion distance is not long, and it is normally about several micrometers. However, the diffusion distance still makes bonding firm under the action of explosive load, because the diffusion rate is very high. It is verified that the bonding strength of the explosive composite plate is high, as described in the following part.

3.3 Mechanical Properties of Composite Plate in AW Condition

3.3.1 Tensile Strength and Fracture Analysis. According to National Standard of the People's Republic of China GB/T 6396-2008 "Clad steel plates-Mechanical and technological test", the tensile strength of the composite plate is tested. The test condition is as follows: the loading rate is 5 mm/min, and the maximal load is 100 kN. During stretching, crack occurs at

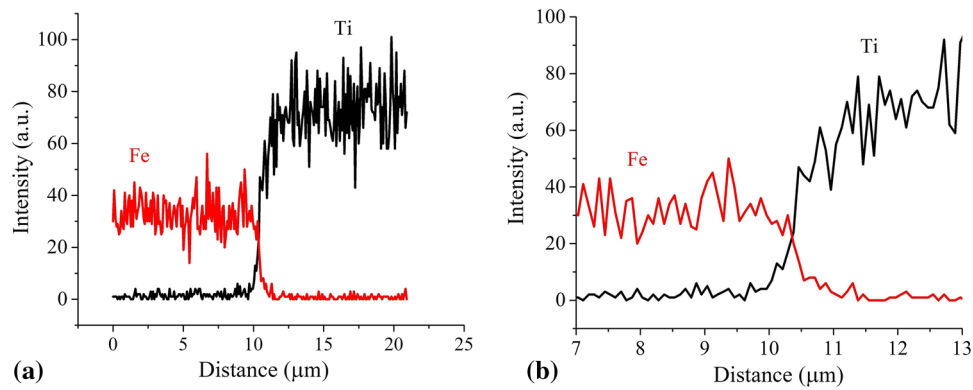


Fig. 5 (a) Line scanning curves of alloying elements and (b) magnification at interface

Table 4 Results of tensile tests for TA10–Q245R composite plate

Sample No.	Tensile strength σ_b , MPa	Elongation δ , %
1	467.83	29.0
2	463.11	29.9
3	471.17	28.7
Average	467.37	29.2

the side of TA10 with lower tensile strength before the composite plate fractures. Simultaneously, the detachment of interface between the base plate and the flyer plate is generated due to great difference in mechanical properties between TA10 and Q245R. The integral fracture of the composite plate finally occurs with the increase in tensile load. The results of tensile tests are shown in Table 4.

From Table 4, the difference among three measurements is relatively slight, and the average tensile strength of the composite plate is 467.37 MPa, and the average elongation is 29.2%. Because the composite plate consists of two different metals such as titanium and steel, the theoretical tensile strength of composite plate is different from that of titanium and of steel. The tensile strength of composite plate is related not only to the strength of base plate and of flyer plate, but also their thickness. The theoretical tensile strength of the composite plate can be calculated through the following equation.

$$\sigma_c = \frac{\sigma_{bL}a_b + \sigma_{fL}a_f}{a_b + a_f} \quad (\text{Eq 1})$$

where σ_c is the theoretical tensile strength of composite plate, MPa; a_b and a_f are the thickness of base plate and flyer plate, respectively, mm; σ_{bL} and σ_{fL} are the low limit values of tensile strength for base plate and flyer plate, respectively, MPa. The values of σ_{bL} and σ_{fL} are 400 and 345 MPa, respectively. The values of a_b and a_f are 12 and 3 mm, respectively. Equation 1 is substituted with these data, and the theoretical tensile strength of composite plate, 389 MPa, is obtained. Compared with the data in Table 4, the tensile strength of composite plate is not only higher than the lower value of the base plate and the flyer plate, but also higher than the calculation value of theoretical tensile strength. Consequently, the tensile strength of composite plate is high enough to satisfy the requirement of tensile property in practical application.

The interfacial bonding state can be reflected by the tensile fracture morphology. SEM analysis of tensile fracture is conducted to the composite plate, and the fracture images are shown in Fig. 6. The interface morphology presents obviously wavy bonding, and detachment occurs at the interface after stretching, as shown in Fig. 6(a). During stretching, because of great difference in mechanical properties between titanium and steel, the plastic deformation cannot be integrated under the same tensile stress, and consequently, the extra stress which is vertical to the interface is generated. With the increase in deformation, the stress along vertical direction also increases. When the extra stress is higher than the interfacial bonding strength, tearing occurs, and detachment is generated.

SEM images of tensile fracture at the sides of TA10 and Q245R are shown in Fig. 6(b) and (c), respectively. There are a lot of dimples on the fracture surface, and the dimple is fine and dense. The fracture obviously presents the ductile characteristics. Figure 6(b) shows that there exists the second phase in the dimple at the side of TA10. The stress concentration or strain mismatching between the second phase and the base metal occurs during stretching; thus, the void nucleates at the interface between two phases. With the further increase in tensile load, the void gradually grows up and develops into big void combined with the surrounding holes. Finally, the dimple is generated on the fracture surface, and the ductile fracture occurs to the material. The dimples can effectively absorb the impact energy, and thus, the impact resistance of the material is improved. The obvious plastic deformation occurs both to the base plate and to the flyer plate before fracturing. So it can be concluded that explosive welding does not do great harm to the plasticity and toughness of the base plate and the flyer plate.

3.3.2 Shear Strength and Fracture Analysis. According to National Standard GB/T 6396-2008, the shear sample of the composite plate is prepared. The dimension of the shear sample is shown in Fig. 7, where a_b and a_f represent the thickness of the base plate and of the flyer plate, respectively. The test condition is as follows: the loading rate is 2 mm/min and the maximal load is 50 kN. During shear test, the experimental force is recorded at the moment when fracture or detachment occurs to the interface of composite plate. The shear strength of composite plate is calculated through the following equation.

$$\tau = \frac{F}{S} \quad (\text{Eq 2})$$

where τ is the shear strength, MPa; F is the experimental force of interface fracture, N; S is the bonding area of interface, mm^2 . Tests

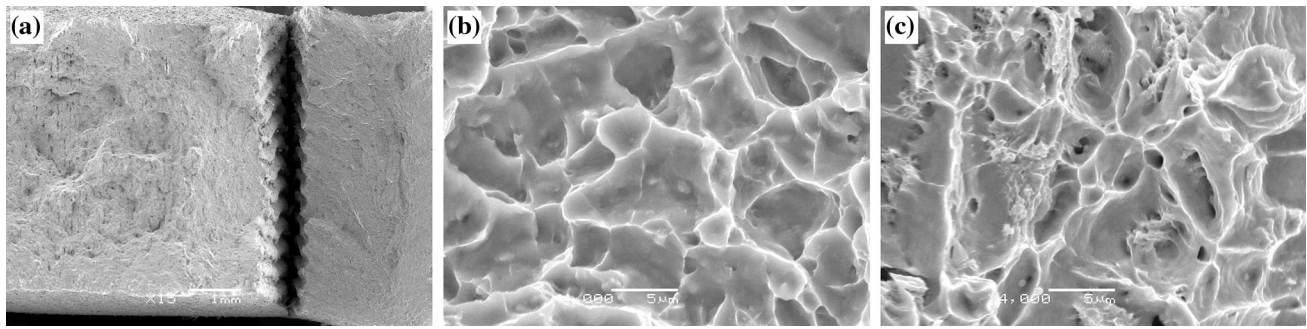


Fig. 6 SEM images: (a) integral fracture, (b) the side of TA10 and (c) the side of Q245R

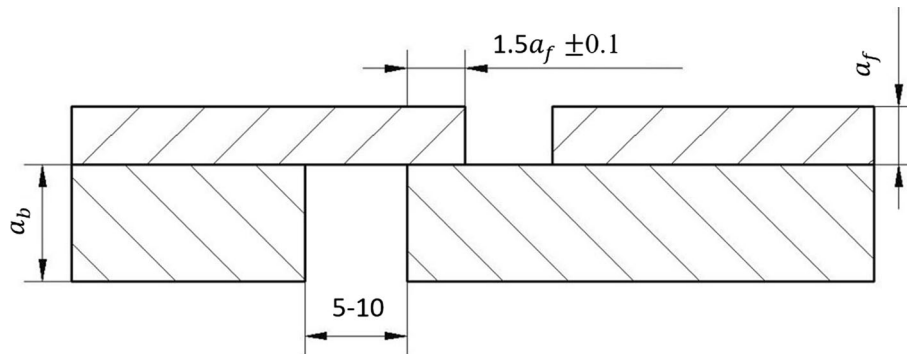


Fig. 7 Dimension of shear sample of composite plate

Table 5 Results of shear experiment for TA10–Q245R composite plate

Sample no.	Thickness of base plate a_b , mm	Thickness of flyer plate a_f , mm	Bonding area S , mm ²	Maximum tensile force F , kN	Shear strength τ , MPa
1	12	3	10.1×4.6	10.20	219.5
2	12	3	10.0×4.5	9.81	218.0
3	12	3	10.1×4.5	9.59	211.0

are carried out for three times, and then, the average is obtained. The results of the shear experiment are shown in Table 5.

The average shear strength of composite plate is 216.2 MPa, which is higher than the given value 196 MPa by National Standard (GB/T 8547-2006). Consequently, it can satisfy the requirement of shear property in practical application. As mentioned above, the effective bonding area at the interface increases due to the wavy bonding; thus, the shear strength of composite plate is relatively high.

SEM images of the shear fracture at the side of Q245R are shown in Fig. 8. The interface presents wavy morphology, and wave peak and trough can clearly be seen, as shown in Fig. 8(a), which is consistent with the previous observation of metallurgical structure (Fig. 1). No defects such as gas pores or impurities are found on the fracture surface. The morphology of shear fracture indicates that the fracture is torn along the interface of composite plate. In addition, the stripes distribute uniformly on the fracture surface, which presents bending morphology. There exists misplacement in some regions, and it is advantageous to inhibit the formation of casting defects in the vortex; thus, the property of composite plate is improved. The morphology of shear fracture is magnified, as shown in Fig. 8(b). Many parallel slip bands are observed on the shear fracture, which demonstrates that obvious slip deformation is

generated before shear fracture. Moreover, the vortex is also found on the fracture, and in the vortex, crack and inclusion are easily produced. Consequently, it is the weak region at the interface of the composite plate. Because the interfacial wavelength is short, the harmful effect caused by the vortex or the melted layer can be greatly reduced.

3.3.3 Bending Property. The dimension of bending sample is 200 mm × 20 mm × 15 mm, and both internal bending and external bending are conducted to the composite plate. At a rate of 1 mm/min, the loading is conducted till cracking occurs at the interface or bending of 180 degrees for the sample. The appearance of the composite plate after bending is shown in Fig. 9. Whether internal or external bending, the detachment does not occur at the interface of the composite plate when the bending angle reaches 180 degrees, and no micro-crack is found (Ref 22). It demonstrates that the composite plate keeps a good combining state, and it can satisfy the requirement for bending property.

3.4 Effect of Heat Treatment on Microstructure and Mechanical Properties of Composite Plate

Heat treatment is carried out for the composite plate, and it can promote the interdiffusion of alloying elements at the interface,

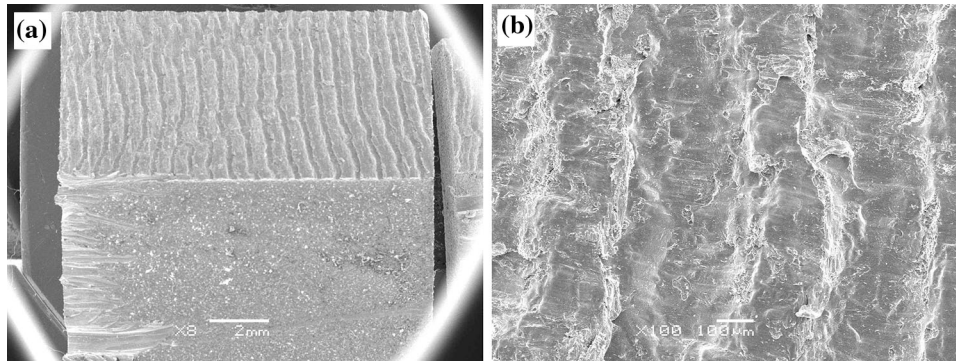


Fig. 8 (a) Morphology of shear fracture and (b) magnification

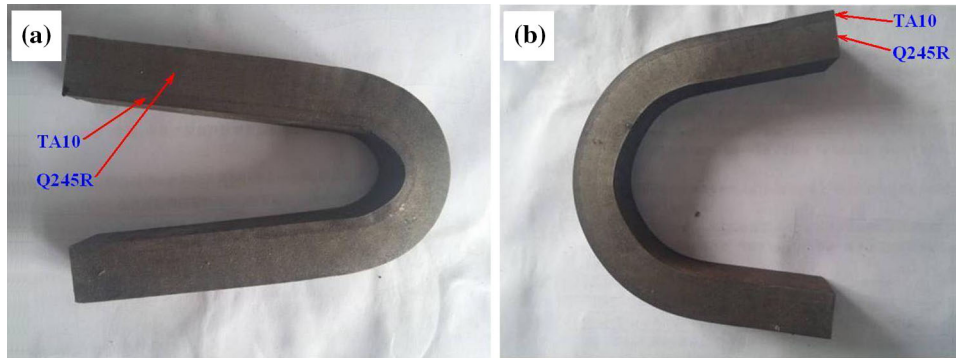


Fig. 9 Appearance of bending samples: (a) internal bending and (b) external bending

which is advantageous to improve the interfacial bonding strength. However, during heat treatment, the brittle intermetallic compound is probably generated at the interface, which results in the decrease in mechanical property (Ref 14, 26). Consequently, the proper heat treatment procedure is very important. Usually, it is expected that the interfacial stress of the composite plate can be eliminated after annealing, and no excessive intermetallic compounds are generated at the interface; thus, the mechanical properties of the composite plate can be improved. As to TA10–Q245R composite plate, the heat treatment is determined by referring to the heat treatment procedure for both the base plate and the flyer plate, and meanwhile, the least of intermetallic compounds are formed at the interface of the composite plate. When the duration time is properly prolonged, recrystallization occurs at the side of TA10, and the interfacial microstructure is improved. After various factors are fully considered (Ref 11, 25), the heat treatment procedure is selected as follows: heating temperature 550, 600, 650 and 700 °C, respectively, duration time 1.5 h, heating rate 10 °C/min, air cooling.

3.4.1 Effect of Heat Treatment on Microstructure at the Side of Steel. After different heat treatments, microstructure of the composite plate is shown in Fig. 10. With the elevation of heating temperature, the microstructural evolution undergoes the following stages, namely streamline structure, disappearance of streamline structure, equiaxed grain, coarse grain, etc. With the disappearance of deformation streamline structure during heat treatment, recrystallization occurs, and the interfacial stress generated by explosive welding is almost eliminated.

During heat treatment process, the metals at both sides of the interface with severe plastic deformation that resulted from

explosive welding undergo the following stages: recovery, recrystallization and grain growth. Recovery occurs immediately when the composite plate is heated, and no incubation period exists at the stage. A lot of dislocations accumulate near the interface of the composite plate after explosive welding. With the elevation of heating temperature, dislocations within the metals continually slip, and local plastic deformation is generated; thus, the stress is eliminated. The course of recrystallization includes nucleation and grain growth. As to the explosive composite plate with great deformation, its nucleation mechanism is based on subgrain, namely with the aid of subgrain within grain. Through subgrain connection or grain growth, the recrystallization nucleus is formed. With the elevation of heating temperature or prolongation of duration time, grain grows up gradually. Because of the greatest deformation at the interface during explosive welding, more energy is stored after deformation. As a result, recrystallization occurs at the interface, as shown in Fig. 10(c). In the present work, recrystallization appears when TA10–Q245R composite plate is heated to 650 °C.

3.4.2 Effect of Heat Treatment on Shear Strength and Tensile Strength of Composite Plate. The shear strength and tensile strength of the composite plate after different heat treatments are given in Table 6. For comparison, the mechanical properties of the composite plate in AW condition are also listed. The shear strength and tensile strength of the composite plate decrease to a certain extent with the elevation of annealing temperature, and both of them are lower than those in AW condition (Ref 26), while the elongation of the composite plate increases with the elevation of annealing temperature. During annealing process, recovery and recrystal-

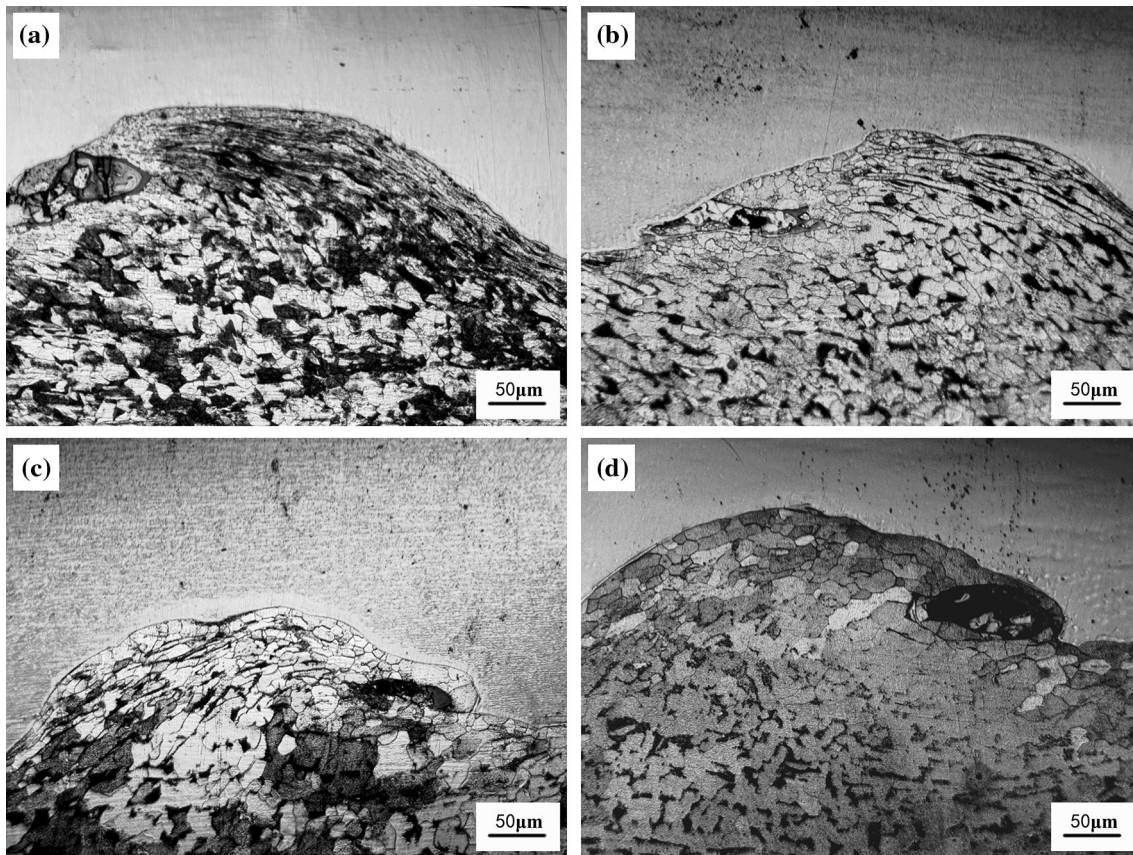


Fig. 10 Interfacial microstructure of composite plate after different heat treatments: (a) 550 °C, (b) 600 °C, (c) 650 °C, (d) 700 °C

Table 6 Tensile strength and shear strength of composite plate after heat treatment

Heating temperature T , °C	Tensile strength σ_b , MPa	Shear strength τ , MPa	Elongation δ , %
AW condition	467.37	216.2	29.2
550	455.65	207.1	31.3
600	442.34	199.1	32.5
650	431.76	187.3	33.9
700	428.77	171.0	34.4

lization of different degrees occur successively to the metals at both sides of the interface, and the dislocation density is greatly decreased within grain or at grain boundary; thus, the explosive strengthening effect at the interface is decreased. When the heating temperature is higher than 600 °C, the shear strength of the composite plate is greatly decreased after heat treatment, which cannot satisfy the requirement of relevant standard (higher than 196 MPa). It is because the carbon and iron atoms migrate from the base plate to the interface, and subsequently, they combine with titanium atom from the flyer plate to form compounds such as Fe_2Ti and TiC during heat treatment, as described in the literature (Ref 11, 25). The brittle compound greatly decreases the property of the bonding interface. On the whole, compared with that in AW condition, the tensile strength of the composite plate does not decrease obviously after heat treatment. It may come from the action of temperature, which promotes the diffusion of alloying elements and increases the

thickness of diffusion layer. The effect of heat treatment on microstructure and mechanical properties of the composite plate should be comprehensively considered, and the suitable heat treatment procedure for TA10–Q245R composite plate is determined as follows: 550 °C \times 1.5 h.

3.4.3 Effect of Heat Treatment on Microhardness at Interface of Composite Plate. The microhardness of the composite plate is measured before and after PWHT. The experimental condition is of load 100 g and duration time 15 s, and the spacing between measurement points is of about 0.2 mm. The distribution curves of microhardness at the interface for the composite plate before and after PWHT are shown in Fig. 11. The hardness value is the highest at the interface (Ref 12), and it is 183.1 HV in AW condition, much higher than that of the base plate and the flyer plate. During explosive welding, the flyer plate impacts the base plate at high speed, and severe plastic deformation occurs to the metal near the interface, which results in work hardening. With the distance away from the interface, the effect of work hardening caused by explosive welding is gradually weakened. Consequently, the microhardness of the metals at both sides of the interface gradually decreases, and it tends to be the original hardness of the base metal. The hardness varies in almost the same way at both sides of the interface. Further analysis reveals that the hardness of the base plate and the flyer plate becomes a constant when the distance is 1 mm away from the interface. It demonstrates that the width of work hardening in two metals caused by explosive welding is almost the same.

In Fig. 11, it can be seen that the hardness decreases to a certain extent at the interface of the composite plate with the

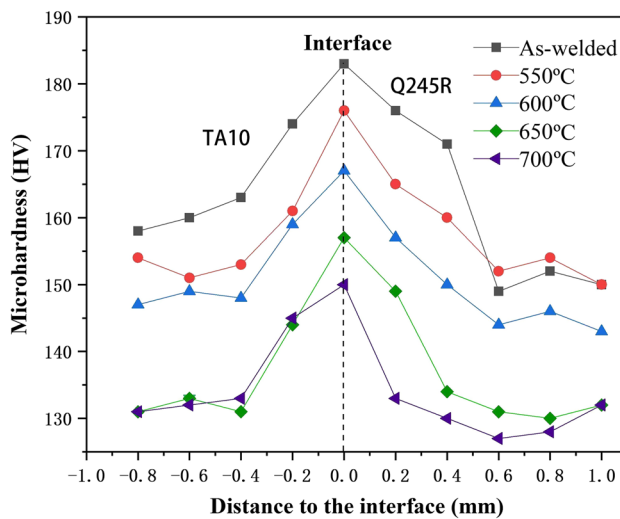


Fig. 11 Distribution curves of microhardness both in AW condition and after PWHT

elevation of heating temperature. When the heating temperature is 550 °C, the hardness greatly decreases at the interface. Because plenty of tangled dislocations at the interface generated by explosive welding undergo recovery, the dislocation density is decreased and the hardness is greatly decreased. Hardness at the side of TA10 near the interface is also greatly decreased, because recrystallization occurs at the side of TA10, and the effect of explosion hardening is weakened. When the heating temperature is 600 °C, hardness is further decreased at both sides of the interface. But the hardness does not decrease obviously in comparison with that at 550 °C. Because although the dislocation density at the interface is decreased at this moment, recrystallization occurs to structure, and the grain becomes small; thus, the effect of grain refinement strengthening is generated. When the heating temperature is 700 °C, the hardness at the side of TA10 is slightly increased. Because carbon atoms at the side of Q245R cross through the interface and diffuse into the side of TA10, the intermetallic compound may be produced at the interface. Hardness at the side of Q245R continuously decreases due to the decarbonization to form ferrite with lower hardness and grain growth.

4. Conclusions

1. The titanium alloy TA10 and the carbon steel Q245R are successfully welded by explosive welding. Microstructure analyses show that the interface of composite plate presents periodic wavy morphology with the formation of front vortex. Plastic deformation is generated to the metals at both sides of the interface. At the side of Q245R, microstructure can be divided into fine-grain zone, streamline structure zone, and base metal zone. TEM analysis indicates that the interfacial width of the composite plate is about 128.77 nm, and the dislocation density within grain at the side of TA10 is higher than that at the side of Q245R.
2. XRD analysis indicates that the main phases at the interface of the composite plate include α -Ti, β -Ti and α -Fe, and no Fe-Ti intermetallic compound phase is found.

Line scanning analysis of alloy elements shows that the interdiffusion is generated between elements Ti and Fe at the interface, and diffusion distance is within micrometers. SEM analysis about tensile fracture demonstrates that there are a lot of equiaxed dimples on the fracture surface of both the base plate and the flyer plate, which presents the obvious characteristic of ductile fracture. SEM observation of the shear fracture shows the wavy morphology uniformly distributes on the fracture surface, and no defects such as gas poles and impurities are found.

3. The average tensile strength of the composite plate is 467.37 MPa, and it is higher than the theoretical tensile strength of 389 MPa. The average shear strength of the composite plate is 216.2 MPa, and it is higher than 196 MPa given by National Standard (GB/T 8547-2006). The composite plate has good bending property, and no detachment nor micro-crack occurs during internal bending or external bending to 180 degrees. Microhardness distribution shows that the hardness is the highest at the interface, and it is 183.1 HV in AW condition. With the distance away from the interface, the hardening effect caused by explosive welding is gradually weakened. Consequently, the hardness is gradually decreased, and it tends to be the original hardness of the base metal.
4. The interfacial microstructure of the composite plate is obviously changed after PWHT. With the elevation of heating temperature, recovery, recrystallization and grain growth occur successively at the side of steel Q245R. After PWHT, both the tensile strength and shear strength of the composite plate are decreased to a certain extent. The suitable heat treatment procedure for TA10–Q245R composite plate is determined as follows: 550 °C \times 1.5 h.

References

1. M. Acarer, B. Gülenç, and F. Findik, The Influence of Some Factors on Steel/Steel Bonding Quality on There Characteristics of Explosive Welding Joints, *J. Mater. Sci.*, 2004, **39**, p 6457–6466
2. M. Acarer, B. Gülenç, and F. Findik, Investigation of Explosive Welding Parameters and Their Effects on Microhardness and Shear Strength, *Mater. Des.*, 2003, **24**, p 659–664
3. M. Nishida, A. Chiba, K. Imamura, H. Minato, and J. Shudo, Microstructural Modifications in an Explosively Welded Ti/Ti Clad Material: I. Bonding Interface, *Metall. Trans. A*, 1993, **24**, p 735–742
4. M. Acarer and B. Demir, An Investigation of Mechanical and Metallurgical Properties of Explosive Welded Aluminium-Dual Phase Steel, *Mater. Lett.*, 2008, **62**, p 4158–4160
5. N. Kahraman and B. Gülenç, Microstructural and Mechanical Properties of Cu-Ti Plates Bonded through Explosive Welding Process, *J. Mater. Process. Technol.*, 2005, **169**, p 67–71
6. R. Kacar and M. Acarer, An Investigation on the Explosive Cladding of 316L Stainless Steel-DIN-P355GH Steel, *J. Mater. Process. Technol.*, 2004, **152**, p 91–96
7. P. Mastanaiah, G.M. Reddy, K.S. Prasad, and C.V.S. Murthy, An Investigation on Microstructures and Mechanical Properties of Explosive Cladded C103 Niobium Alloy over C263 Nimonic Alloy, *J. Mater. Process. Technol.*, 2014, **214**, p 2316–2324
8. C.X. Sun, S.M. Wang, W.H. Guo, W.P. Shen, and C.C. Ge, Bonding Interface of W-CuCrZr Explosively Welded Composite Plates for Plasma Facing Components, *J. Mater. Sci. Technol.*, 2014, **30**, p 1230–1234

9. J. Song, A. Kostka, M. Veehmayer, and D. Raabe, Hierarchical Microstructure of Explosive Joints: Example of Titanium to Steel Cladding, *Mater. Sci. Eng. A*, 2011, **528**, p 2641–2647
10. Z.Y. Zhang, L. Peng, J.M. Wang, Y. Li, and R.S. Liu, Study on Defects of Large-Sized Ti/Steel Composite Materials in Explosive Welding, *Procedia Eng.*, 2011, **16**, p 14–17
11. T.N. Prasanthi, C.S. Ravikiran, and S. Saroja, Explosive Cladding and Post-weld Heat Treatment of Mild Steel and Titanium, *Mater. Des.*, 2016, **93**, p 180–193
12. N. Kahraman, B. Gülenç, and F. Findik, Joining of Titanium/Stainless Steel by Explosive Welding and Effect on Interface, *J. Mater. Process. Technol.*, 2005, **169**, p 127–133
13. S.A.A. Akbari-Mousavi and P.F. Sartangi, Experimental Investigation of Explosive Welding of CP-Titanium/AISI 304 Stainless Steel, *Mater. Des.*, 2009, **30**, p 459–468
14. S.A.A. Akbari-Mousavi and P.F. Sartangi, Effect of Post-weld Heat Treatment on the Interface Microstructure of Explosively Welded Titanium-Stainless Steel Composite, *Mater. Sci. Eng. A*, 2008, **494**, p 329–336
15. S.A.A. Akbari-Mousavi, L.M. Barrett, and S.T.S. Al-Hassani, Explosive Welding of Metal Plates, *J. Mater. Process. Technol.*, 2008, **202**, p 224–239
16. P. Manikandan, K. Hokamoto, M. Fujita, K. Raghukandan, and R. Tomoshige, Control of Energetic Conditions by Employing Interlayer of Different Thickness for Explosive Welding of Titanium/304 Stainless Steel, *J. Mater. Process. Technol.*, 2008, **195**, p 232–240
17. K. Raghukandan, Analysis of the Explosive Cladding of Cu-Low Carbon Steel Plates, *J. Mater. Process. Technol.*, 2003, **139**, p 573–577
18. A. Durgutlu, B. Gülenç, and F. Findik, Examination of Copper/Stainless Steel Joints Formed by Explosive Welding, *Mater. Des.*, 2005, **26**, p 497–507
19. A. Durgutlu, H. Okuyucu, and B. Gülenç, Investigation of Effect of the Stand-off Distance on Interface Characteristics of Explosively Welded Copper and Stainless Steel, *Mater. Des.*, 2008, **29**, p 1480–1484
20. S.A.A. Akbari-Mousavi, S.T.S. Al-Hassani, and A.G. Atkins, Bond Strength of Explosively Welded Specimens, *Mater. Des.*, 2008, **29**, p 1334–1352
21. B. Wronka, Testing of Explosive Welding and Welded Joints. The Microstructure of Explosive Welded Joints and Their Mechanical Properties, *J. Mater. Sci.*, 2010, **45**, p 3465–3469
22. N.V. Rao, G.M. Reddy, and S. Nagarjuna, Structure and Properties of Explosive Clad HSLA Steel with Titanium, *Trans. Indian Inst. Met.*, 2014, **67**, p 67–77
23. I.N. Maliutina, A.A. Bataev, I.A. Bataev, K.A. Skorokhod, and V.I. Mail, Explosive Welding of Titanium with Stainless Steel Using Bronze-Tantalum as Interlayer, *The 9th International Forum on Strategic Technology (IFOST)*, p 436–439
24. I.N. Maliutina, V.I. Mali, K.A. Skorokhod, and A.A. Bataev, Effect of Heat-Treatment on the Interface Microstructure of Explosively Welded Stainless Steel-Bronze Composite, *Appl. Mech. Mater.*, 2015, **698**, p 495–500
25. H.T. Jiang, X.Q. Yan, J.X. Liu, and X.G. Duan, Effect of Heat Treatment on Microstructure and Mechanical Property of Ti-Steel Explosive-Rolling Clad Plate, *Trans. Nonferrous Met. Soc. China*, 2014, **24**, p 697–704
26. M. Yadegari, A.R. Ebrahimi, and A. Karami, Effect of Heat Treatment on Interface Microstructure and Bond Strength in Explosively Welded Ti/304L Stainless Steel Clad, *Mater. Sci. Technol.*, 2013, **29**, p 69–75
27. G.S. Zhang, S.Z. Hou, S.Z. Wei, J.W. Li, and L.J. Xu, Effects of Aging Treatment on Performance of Explosive Welded Beryllium-Bronze/Carbon-Steel Composite Plate, *Appl. Mech. Mater.*, 2011, **117–119**, p 862–865
28. W. Deng, M. Lu, X.J. Tian, and R.X. Dai, Experimental and Interfacial Waveform Investigation on Aluminum/Stainless Steel Composite Tube by Explosive Welding, *Adv. Mech. Eng. Appl.*, 2013, **3**, p 304–308
29. P. Muneshwar, S.K. Singh, K.N. Kumar, B. Pant, and K. Sreekumar, Metallurgical Studies on Explosive Welded Aluminium Alloy-Stainless Steel Bimetallic Plates, *Mater. Sci. Forum*, 2012, **710**, p 644–649
30. M. Acarer, Electrical, Corrosion, and Mechanical Properties of Aluminum-Copper Joints Produced by Explosive Welding, *J. Mater. Eng. Perform.*, 2012, **21**, p 2375–2379
31. H.B. Xia, S.G. Wang, and H.F. Ben, Microstructure and Mechanical Properties of Ti/Al Explosive Cladding, *Mater. Des.*, 2014, **56**, p 1014–1019
32. S.G. Wang, H.B. Xia, X.M. Han, and Y. Huang, Microstructure and Mechanical Properties of Ti-Al Explosive Composite Plate After Heat Treatment, *Adv. Eng. Res.*, 2015, **41**, p 534–540
33. F. Findik, Recent Developments in Explosive Welding, *Mater. Des.*, 2011, **32**, p 1081–1093

Publisher's Note Springer Nature remains neutral with regard to jurisdictional claims in published maps and institutional affiliations.